

Testing antimatter gravity with muonium

KLAUS KIRCH

*Institute for Particle Physics, ETH Zurich and
Paul Scherrer Institute, Switzerland.*

klaus.kirch@psi.ch

KIM SIANG KHAW

Institute for Particle Physics, ETH Zurich, Switzerland.

khaw@phys.ethz.ch

The debate about how antimatter or different antimatter systems behave gravitationally will be ultimately decided by experiments measuring directly the acceleration of various antimatter probes in the gravitational field of the Earth or perhaps redshift effects in antimatter atoms caused by the annual variation of the Sun's gravitational potential at the location of the Earth. Muonium atoms may be used to probe the gravitational interaction of leptonic, second generation antimatter. We discuss the progress of our work towards enabling such experiments with muonium.

Keywords: Antimatter gravity, muonium, spectroscopy, Mach Zehnder interferometer, muon spin rotation, superfluid helium, phase space compression

PACS numbers : 03.75.Dg, 04.80.Cc, 29.25.-t, 36.10.Ee, 41.75.Ak, 52.80.Dy, 67.25.D-, 76.75.+i

1. Introduction

The equivalence of the gravitational and the inertial mass of macroscopic test masses of ordinary matter has been tested to very high precision, e.g. with a differential measurement of Be and Ti masses using a highly sophisticated torsion balance ¹. Gravitational acceleration of ordinary matter atoms in the Earth gravitational field has also been measured to high precision, e.g. using atom interferometry methods ^{2,3}. Neutral kaon oscillations have been used to set very tight constraints on differences in the gravitational interaction of their constituents, see e.g. ⁴ and arguments have been extended using all neutral meson oscillations ⁵. While it may therefore be very improbable to find some general 'antigravity', similar arguments as put forward already in ⁶ can still be applied and the gravitational interaction may perhaps be much more complex and allow for cancellations in some systems. A first crude limit has been set on the antihydrogen gravitational acceleration ⁷, however, neither decisive yet in its magnitude nor in its sign. The precise measurement of antimatter gravity in various systems may serve as an important input for constructing theories of quantum gravity and it could potentially provide insights to dark matter and dark energy which remain mysterious until today.

Muonium (Mu) is the hydrogen like bound state of μ^+ and e^- . It has been studied extensively since the 1960s to test bound state QED, to determine fundamental parameters and to search for exotic physics^{8,9,10}. It can be reliably calculated within QED because it is purely leptonic and essentially free of hadronic effect. It can live relatively long, limited by the muon life time ($\tau_\mu = 2.2 \mu\text{s}$). Its 1S-2S transition frequency^{11,12} and the hyperfine splitting of the ground state¹³ have been measured to high precision (4 ppb and 12 ppb).

In recent years, there is a renewed interest in physics with Mu atoms, triggered by new ideas for much improved slow muon and muonium beams and by progress in laser technology. Measuring Mu's gravitational interaction with ordinary matter would be complementary to such measurements with antihydrogen and positronium and would be the first test for this second generation leptonic system where the mass is dominated by the heavy μ^+ .

Two very different approaches for a Mu gravity experiment are being considered:

- Search for an annual modulation of the Mu(1S-2S) transition frequency¹⁴
- Use a high quality Mu beam passing through a Mach Zehnder atom interferometer^{15,16,17,18}

Our group is pursuing research into both directions and developing the necessary experimental prerequisites. Some technical challenges and the current situation of research and development will be sketched in the following sections.

2. Experimental challenges

2.1. 1S-2S spectroscopy

First proposed for positronium 1S-2S spectroscopy^{14,19}, the main idea of this method is to utilize the gravitational redshift, where the frequency of a photon is changed depending on the gravitational potential. When the Earth is orbiting the Sun, their distance varies by about 5.0×10^6 km during the year, corresponding to 3.2×10^{-10} in terms of relative frequency shift¹⁴. Hence, a precision level of about 0.1 ppb is needed to be sensitive to an effect which could shift the Mu transition frequency with respect to a frequency reference based on an ordinary matter system. The required sensitivity implies a 40-fold improvement in the measurement of Mu 1S-2S transition frequency.

This improvement requires: a) highest possible slow μ^+ rate (e.g., $4000\mu^+/\text{s}$ at LEM^{20,21} facility at PSI), b) highest possible $\mu^+ \rightarrow$ slow Mu conversion rate (e.g., Mesoporous silica²²), c) high power continuous wave laser (based on the development of, e.g., Ps 1S-2S at ETHZ¹⁹) and d) a better known reference frequency (e.g., I_2 calibration via frequency comb²³).

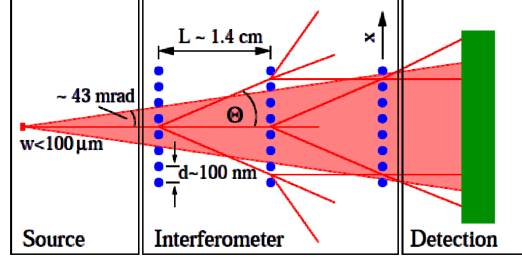


Fig. 1. Mach Zehnder interferometer for muonium atom.

2.2. Mach Zehnder interferometer

Interferometry methods can be very sensitive and it was proposed to measure the phase shift of neutral antimatter caused by the Earth's gravitational field in a transmission-grating interferometer^{15,16,17,18} (see Fig. 1). To apply this technique to Mu and in order to have enough statistics and a measurable deflection, one should aim for: a) separation between gratings $\geq 2.2 \mu\text{s}$, b) free standing grating pitch $\approx 100 \text{ nm}$ and c) $\geq 10^5/\text{s}$ mono-energetic Mu beam (based on a superfluid helium source).

The precision of this method could reach $\frac{0.3g}{\sqrt{\#\text{days}}}$ and one could hope for 3% from a 100 day measurement.

3. Current status of our R&D

3.1. 1S-2S spectroscopy

3.1.1. Mu production with porous silica

For high precision spectroscopy Mu in vacuum is needed to avoid matter effects. Bulk silica has a high Mu formation rate but no emission from the target. Silica with structured pore-networks (porous silica) could lead to a high fraction of Mu diffusing out into vacuum (see Fig. 2).

Measurements have been carried out²² at PSI's LEM with $4000/\text{s} \mu^+$ on the sample. A muon spin rotation technique was used to extract the Mu formation rate and a positron shielding technique allowed to extract the Mu yield in vacuum.

3.1.2. Muon spin rotation technique (μSR)

Due to parity violation of the weak interaction, decay positrons are emitted preferentially in direction of μ^+ spins. By monitoring the evolution of μ^+ spins after implantation in an external magnetic field, unbound μ^+ and Mu can be distinguished because the Larmor precession frequency of Mu is about 100 times larger than that of μ^+ .

With segmented positron detectors around the target, the Mu formation rate

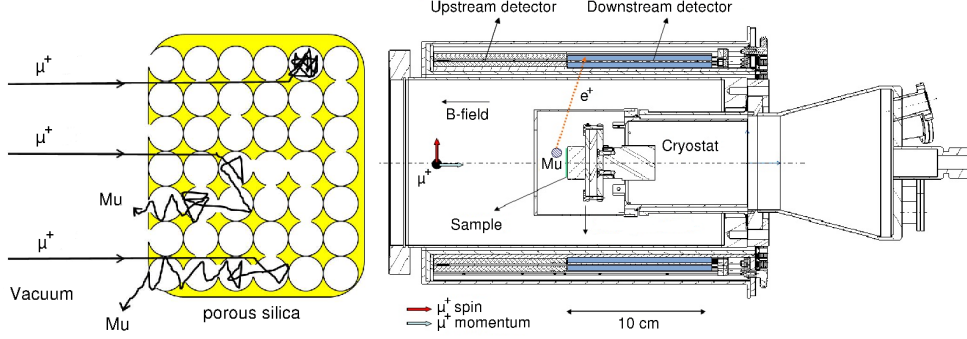


Fig. 2. (left) Porous film of $1\ \mu\text{m}$ thickness, a pore size of $5.0\pm 0.5\ \text{nm}$, and a density of $1.1\ \text{g/cm}^3$. (right) LEM sample chamber. The sample is glued on a silver coated copper mount contacted to a cryostat. The sample is surrounded by scintillators for positron detection grouped in upstream and downstream counters. Each of them is additionally segmented in top, bottom, left and right.

can be determined from the disappearance of the μ^+ precession signal.

3.1.3. Positron shielding technique (PST)

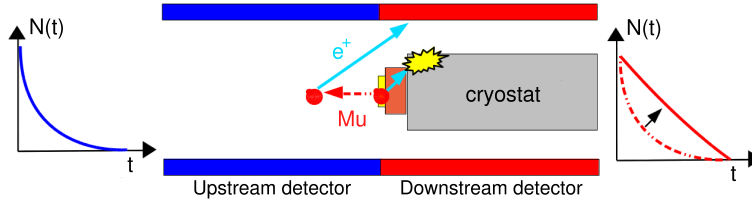


Fig. 3. A schematic illustration of positron shielding technique (PST).

Without Mu emission into vacuum an exponential decay curve is observed with the downstream detector. When there is Mu emission into vacuum, a deviation from the exponential curve appears due to less shielding when Mu decay outside of the sample (see Fig. 3).

GEANT4 ²⁴ simulations were done for 0% emission (F_0) and 100% emission (F_{100}) and the data were fitted with $F_{fit} = aF_{100} + (1 - a)F_0$, where a is the Mu yield in vacuum. A typical result is shown in Fig. 4(left).

3.1.4. Mu yield in vacuum

We have studied the Mu yield in vacuum for different pore sizes and temperatures. The best results obtained so far are 20% at 100 K and 40% at 250 K for 5 nm pore

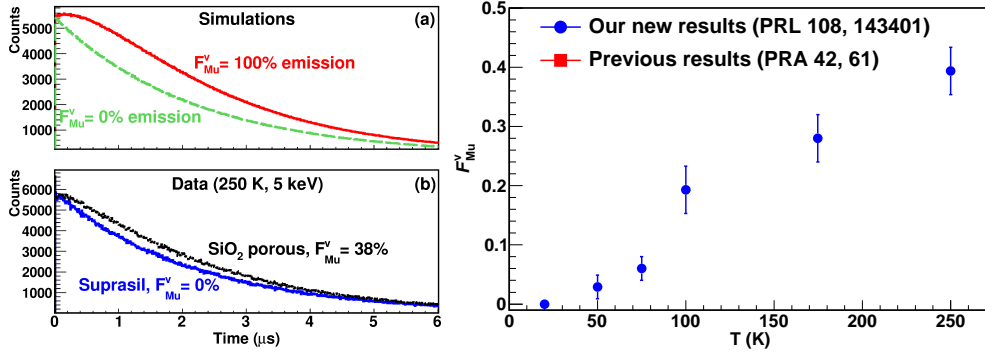


Fig. 4. (left) Simulated (a) and measured (b) positron spectra. A fit function is used to extract the Mu yield in vacuum. 38% was obtained for porous silica and 0% was obtained for suprasil (fused quartz) where zero Mu vacuum yield is expected. (right) A temperature dependence of Mu vacuum yield for porous silica F-sample.

size (see Fig. 4). There is evidence that a Boltzmann velocity distribution for Mu is preferred over a uniform velocity distribution.

With these vacuum yields and available laser technology, it appears possible to improve precision in the Mu 1S-2S frequency by a factor of 10.

3.2. Mu atom interferometry

Before being able to apply a Mach-Zehnder interferometer to a Mu beam, such a beam must be developed. It will be based on a much improved slow muon beam and a novel Mu production and extraction to vacuum from superfluid helium.

3.2.1. Slow muon beam

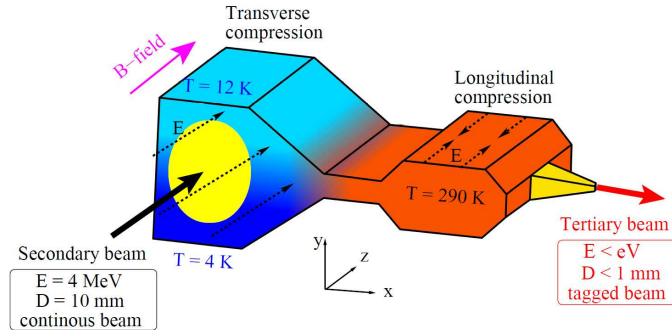


Fig. 5. A schematic illustration of phase space compression.

Phase space compression by a factor of 10^{10} compared to a standard surface muon beam can be achieved by stopping muons in a few mbar of He gas, compressing the stop distribution and extracting them back to vacuum²⁵. The compression uses a position-dependent μ^+ drift in E and B fields in helium gas. The final ultra slow μ^+ beam with sub-mm size and sub-eV energy can be re-accelerated (see Fig. 5).

The compression scheme is divided into 3 stages: transverse compression, longitudinal compression and extraction of the μ^+ beam. The efficiency of the scheme is estimated to about 0.1%, mainly limited by the muon lifetime.

3.2.2. Longitudinal compression

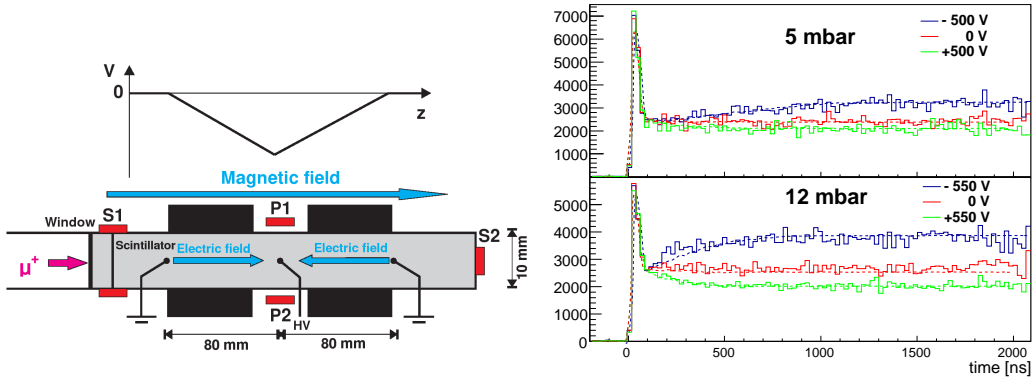


Fig. 6. (left) A schematic illustration of longitudinal compression. (right) Measured (continuous lines) and simulated (dotted) positron spectra divided by $e^{-t/2200}$ for (+550 V, 0 V, -550 V) electric fields at 5 mbar and 12 mbar helium gas pressure.

Longitudinal compression was demonstrated at PSI's π E1 beam line using μ^+ of 10 MeV/c at a rate of $2 \times 10^4/\text{s}$ (see Fig. 6). Low energy μ^+ elastic collision physics and Mu formation in helium gas, which were scaled from available data for protons^{27,28}, were implemented into GEANT4, and simulations were done to compare with the data. In Fig. 6 (right), time spectra of detected positrons at P1 and P2 are displayed after a μ^+ trigger in S1. To eliminate lifetime effects, the spectra were divided by e^{-t/τ_μ} transforming an exponential decay to a uniform distribution. When μ^+ are drifting to the central region, the detection efficiency and count rate increase, as is seen for negative voltage. The opposite effect occurs when the polarization of the electric field is reversed. Good agreement between simulation and data was achieved and compression of the 16 cm wide muon swarm into 0.5 cm width occurs in much less than $2 \mu\text{s}$. This result shows that the compression process is faster than the mean lifetime of μ^+ and hence the longitudinal compression is feasible²⁶.

3.2.3. Helium gas density gradient

One challenge of the transverse compression part is to realize a helium gas density gradient over the muon stop distribution via a static temperature gradient. Turbulence must be avoided by operating the lower side of the target at lower temperature.

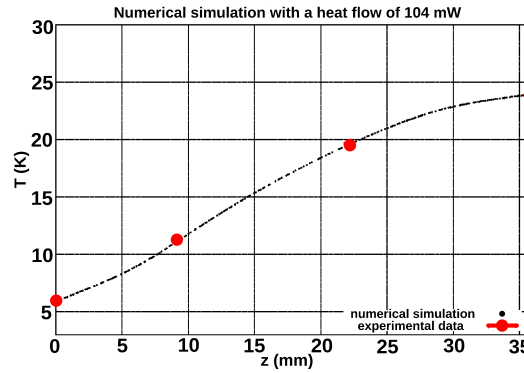


Fig. 7. Comparison of simulation and measurements of the gas cell with density gradient.

We have made a first demonstration of a stationary temperature gradient in the laboratory. A cylinder made of copper (top, bottom) and thin stainless steel (sides) was attached to a cryostat and equipped with thermometry and heaters. The cylinder was filled with helium pressures of 0.01 mbar to 50 mbar and stationary temperatures have been measured and simulated. Good agreement between a COMSOL simulation and measured data was obtained²⁹ (see Fig. 7 for an example) proving the feasibility for a muon target assembly.

4. Conclusion and Outlook

So far our feasibility studies into Mu production for 1S-2S spectroscopy and for atom interferometry yield very promising results. High Mu vacuum yields have been demonstrated for suitable porous silica targets opening up the path for a next generation spectroscopy experiment. Towards a high quality slow μ^+ beam, longitudinal compression has been demonstrated and the feasibility for a gas target with helium density gradient was shown. The next step for the beam development will be the demonstration of transverse compression of a muon stop distribution. In a separate experiment we aim at remeasuring the Mu production in superfluid helium below 0.5 K³⁰ and verify the predicted quasi-monoenergetic emission into vacuum^{31,32}. Studies of a Mach-Zehnder interferometer will be pursued in collaboration with IIT¹⁸.

Acknowledgments

This work was performed at the ETH Zurich and at the Paul Scherrer Institut. We gratefully acknowledge the support of the accelerator and beamline groups. Our work greatly benefitted from using the μ E4 LEM installation and the new π E1 area and intense collaboration with Thomas Prokscha, Konrad Deiters and Claude Petitjean, the ETH group Precision Physics at Low Energy and the PSI Muon Physics Group. We would like to thank Aldo Antognini, Paolo Crivelli, Dan Kaplan, Tom Phillips, Florian Piegsa, and David Taquu for fruitful discussions in connection with this conference presentation. This work was supported by the Swiss National Science Foundation grants 200021-129600 and 200021-146902.

References

1. S. Schlamminger *et al.*, *Phys. Rev. Lett.* **100**, 041101 (2008).
2. N. Poli *et al.*, *Phys. Rev. Lett.* **106**, 038501 (2011).
3. R. Charriere *et al.*, *Phys. Rev. A* **85**, 013639 (2012).
4. A. Apostolakis *et al.*, *Phys. Lett. B* **452**, 425 (1999).
5. S. G. Karshenboim, *arXiv:0811.1009 [gr-qc]* (2008).
6. M. M. Nieto and T. Goldman, *Phys. Rep.* **205**, 221 (1991).
7. A. E. Charman *et al.*, *Nature Communication* **4**, 1785 (2013).
8. V. W. Hughes, *Ann. Rev. Nucl. Sc.* **16**, 445 (1966).
9. K. Jungmann, *Nucl. Phys.* **B155**, 355 (2006).
10. S. G. Karshenboim, *Phys. Rep.* **422**, 1 (2005).
11. S. Chu *et al.*, *Phys. Rev. Lett.* **60**, 101 (1988).
12. V. Meyer *et al.*, *Phys. Rev. Lett.* **84**, 1136 (2000).
13. W. Liu *et al.*, *Phys. Rev. Lett.* **82**, 711 (1999).
14. S. G. Karshenboim, *arXiv:0811.1008 [gr-qc]* (2008).
15. L. M. Simons, *Private Communication* (1995).
16. T. Phillips, *Hyperfine Interactions* **109**, 357 (1997).
17. K. Kirch, *arXiv:physics/0702143 [physics.atom-ph]* (2007).
18. D. Kaplan *et al.*, *arXiv:1308.0878 [physics.ins-det]* (2013).
19. P. Crivelli *et al.*, *Canadian Journal of Physics* **89(1)**, 29-35 (2011).
20. E. Morenzoni *et al.*, *Physica B* **289-290**, 653 (2000).
21. T. Prokscha *et al.*, *Nucl. Instr. Meth. A* **595**, 317 (2008).
22. A. Antognini *et al.*, *Phys. Rev. Lett.* **108**, 143401 (2012).
23. I. Fan *et al.*, *Phys. Rev. A* **89**, 032513 (2014).
24. S. Agostinelli *et al.*, *Nucl. Instr. Meth. A* **505**, 250 (2003).
25. D. Taquu *Phys. Rev. Lett.* **97**, 194801 (2006).
26. Yu Bao *et al.*, *Phys. Rev. Lett.* **112**, 224801 (2014).
27. M. Senba, *J. Phys. B: Atom. Molec. Phys.* **22**, 2027 (1989).
28. P. S. Krstic and D. R. Schultz, *Atomic and Plasma-Material Interaction Data for Fusion 8* (1998).
29. G. Wichmann, *Stationary Density Gradient in a Helium Gas Cell at Low Temperature, ETH Master Thesis, Spring 2013* (2013).
30. R. Abela *et al.*, *JETP Lett.* **57**, 157 (1993).
31. M. Saarela and E. Krotscheck, *JLTP* **90**, 415 (1993).
32. D. Taquu and E. Krotscheck, *Private Communication* (2013).